Ballooning-mode stability of shaped high-β tokamaks

A. K. Agarwal, S. N. Bhattacharyya, and A. Sen
Institute for Plasma Research, Bhat, Gandhinagar-382424, India
(Received 17 March 1993; revised manuscript received 22 October 1993)

The effect of elongation and triangularity of flux surfaces on the local and global stability of high-n ideal ballooning modes in a high-β tokamak are investigated. The equilibrium surfaces are obtained by a numerical solution of the Grad-Shafranov equation using an efficient algorithm based on a generalized variational technique. A marginal stability analysis of these surfaces is carried out in which the equilibrium shift, elongation, triangularity, and their radial variations are taken into account. The influence of the cylindrical safety factor (q_c), as well as the variations in the shape of β and q profiles, on the maximum attainable beta value (β_c) are also considered. Detailed numerical results, over a wide range of parameter space, show that the effect of boundary elongation κ_a is always stabilizing while the effect of boundary triangularity δ_a depends on the values of κ_a and q_c. It is found that for elongated cross section ($\kappa_a \geq 1.6$), the effect of δ_a is always stabilizing. We present an alternative scaling law that effectively captures these features of the shape parameter dependences. For a JET (Joint European Torus) -type plasma, broad β profiles and q profiles that tend to be flat in the interior are found to be favorable for achieving a high β_c value.

PACS number(s): 52.35.Py, 52.55.Fa, 52.30.Bt

I. INTRODUCTION

It has been well established both theoretically [1–3] and experimentally [4,5] that the high-n ideal ballooning modes play a crucial role in limiting the plasma β value in tokamaks (where n is the toroidal mode number and β is the ratio of the plasma pressure to the magnetic-field pressure). Among the various factors that influence the stability of these modes, the effect of the shape of the plasma boundary has received attention in some recent studies [6–10]. Kwon and Hender [6] have examined the role of the plasma shape in gaining accessibility to the second ballooning stability regime. In *D* III-*D* (doublet III-*D*) experiment [7], a record high β of 11% has been achieved by taking a *D*-shaped plasma boundary with elongation $\kappa_a = 2.34$. The effect of the triangularity of the plasma boundary on the β limit set by ideal ballooning modes has also been studied in [8–10] for typically high values of boundary elongation ($\kappa_a \geq 1.9$). In general the effect of triangularity is found to be stabilizing. A simple scaling law for the maximum β for marginal stability to high-n ballooning modes has been obtained in [11] in terms of elongation κ_a, q_c and aspect ratio A. Some scaling laws incorporating triangularity δ_a have been obtained in [12,13]. The scaling laws are usually valid over a limited parameter range. Nevertheless they emphasize the fact that the plasma geometry, as well as the β and q profiles, play an important role in determining the maximum achievable β, and much further work needs to be done to elucidate the complex dependencies on these factors. The present work is motivated by such a consideration, and we investigate in detail the effect of elongation ($1 \leq \kappa_a \leq 2$), triangularity ($0 \leq \delta_a \leq 0.2$), and the modified edge safety factor q_c [defined in terms of (current)/(area)] on β_c using typical forms for β and q profiles. We also consider variations in the shape of the β and q profiles for a specific case of a JET (Joint European Torus) -type plasma boundary in order to study their influence on the overall global stability. We find that the effect of triangularity δ_a is not always stabilizing, but depends on κ_a and q_c values. The detailed dependencies are elucidated by an extensive numerical study of the local stability of ballooning modes on various flux surfaces, and over a wide range of parameter values. A unified scaling law capturing these features is presented. It may be noted that the shape of the flux surfaces depend not only on the boundary shape but can also be influenced by other factors such as sheared equilibrium plasma flows [14,15]. Thus our study could have some relevance for stability of equilibria with flows.

The paper is organized as follows. In Sec. II we discuss the equilibrium solution of the Grad-Shafranov equation in the high-β tokamak limit. The method is based on a variational formulation and yields a set of ordinary differential equations which are numerically solved for the shift, elongation, and triangularity of the equilibrium flux surfaces. The ballooning-mode stability equation for these surfaces is written down in Sec. III, and its method of solution discussed. The results from local and global stability analysis and a unified scaling law are presented and discussed in Sec. IV.

II. VARIATIONAL EQUILIBRIUM

We adopt a variational formulation to compute the plasma equilibrium of a high-β tokamak plasma. This approach was first used by Choe and Freidberg [16] to calculate arbitrarily large Shafranov shifts of circular flux surfaces and to study their effect on ballooning-mode stability. Mauel [17] extended this analysis to calculate both the shift and elliptic elongation of the flux surfaces. In our formulation we further generalize the method to include the triangularity of the flux surfaces. A major advantage of the variational formulation is that it obviates the need to solve a partial differential equation, and

reduces the equilibrium problem to the solution of a set of ordinary differential equations. It thus provides for a simple and efficient computational solution, which is also reasonably accurate when compared to direct numerical solutions of the Grad-Shafranov equation. The variational approach also leads to direct computations of the profiles (and the radial derivatives) of the Shafranov shift, elongation, and triangularity of equilibrium flux surfaces. These quantities are of direct relevance to the stability analysis.

Following Choe and Freidberg [16], we adopt the high-β tokamak ordering ($\beta_\phi \sim \epsilon$, $\beta_p \sim 1/\epsilon$, $q \sim 1$, where $\epsilon = a/R_0$ is the inverse aspect ratio), in which the Grad-Shafranov equation for the tokamak equilibrium reduces to

$$\nabla^2\psi + R_0(R-R_0)\frac{d\beta}{d\psi} + \frac{d\Gamma}{d\psi} = 0 , \tag{1}$$

where ψ is the poloidal flux function, R is the distance from the symmetry axis, R_0 is the major radius, and $\beta(\psi)$ and $\Gamma(\psi)$ are free functions of ψ related to the plasma pressure and current, respectively. Equation (1) is equivalent to the variational principle $\delta L = 0$, where

$$L = \int\int \{\tfrac{1}{2}|\nabla\psi|^2 - R_0(R-R_0)\beta(\psi) - \Gamma(\psi)\} dR\, dZ . \tag{2}$$

Z is the vertical coordinate in the direction of symmetry axis, and the integration is over the entire plasma cross section. In order to describe equilibria with D-shaped surfaces, we introduce flux coordinates (r,θ) defined by

$$\begin{aligned} R &= R_0 + \sigma(r) + r\cos\theta , \\ Z &= r\kappa(r)[\sin\theta - \delta(r)\sin 2\theta] , \end{aligned} \tag{3}$$

where σ, κ, and δ represent the shift from the geometric center, elongation, and triangularity of the flux surfaces, respectively, and θ is a periodic coordinate ($0 \le \theta \le 2\pi$, $0 \le r \le a$, a is the horizontal minor radius). In the above definition, κ is not quite the ratio of the vertical to the horizontal diameters, but is slightly smaller (depending on δ) than the usual definition of elongation. Likewise the δ in (3) is approximately half the value of the conventionally defined triangularity parameter [1,6,8]. For example, our parameters $\kappa = 1.6$ and $\delta = 0.17$ correspond to the conventional values of 1.68 and 0.3, respectively (these values are typical of the JET equilibrium). For the particular case of $\kappa(r) = 1$ and $\delta(r) = 0$, Eq. (3) describes the conventional shifted-circle model [16] of equilibrium. In the above equation, r is assumed to be a flux label, so that $\psi = \psi(r)$. Using Eq. (3), the expression for L in Eq. (2) can be written in terms of (r,θ) as

$$L = \pi\int_0^a [r\psi'^2 F/\kappa - (r^2\sigma\kappa)' R_0\beta + (r^3\kappa\delta)' R_0\beta/2 - (r^2\kappa)'\Gamma] dr , \tag{4}$$

where

$$F = \frac{1}{2\pi}\int_0^{2\pi} \frac{b}{X} d\theta , \tag{5}$$

$$b = \sin^2\theta + \kappa^2(\cos\theta - 2\delta\cos 2\theta)^2 , \tag{6}$$

$$X = 1 + \sigma'\cos\theta + \bar{\kappa}\sin^2\theta - 2\delta(\cos\theta + \sigma')\cos 2\theta - (\delta + \delta\bar{\kappa} + r\delta')\sin\theta\sin 2\theta , \tag{7}$$

and $\bar{\kappa} = r\kappa'/\kappa$. Primes denote differentiation with respect to r. For L to be stationary with respect to arbitrary variations in ψ, σ, κ, and δ, we must have

$$2\psi'\left[\frac{r\psi'}{\kappa}F\right]' + (r^2\sigma\kappa)' R_0\beta' - \tfrac{1}{2}(r^3\kappa\delta)' R_0\beta' + (r^2\kappa)'\Gamma' = 0 , \tag{8}$$

$$\left[\frac{r\psi'^2}{\kappa}\frac{\partial F}{\partial\sigma'}\right]' - r^2\kappa R_0\beta' = 0 , \tag{9}$$

$$\left[\frac{r\psi'^2}{\kappa}\frac{\partial F}{\partial\kappa'}\right]' + \frac{r\psi'^2}{\kappa^2}F - \frac{r\psi'^2}{\kappa}\frac{\partial F}{\partial\kappa} - r^2\sigma R_0\beta' + \tfrac{1}{2}r^3\delta R_0\beta' - r^2\Gamma' = 0 , \tag{10}$$

$$\left[\frac{r\psi'^2}{\kappa}\frac{\partial F}{\partial\delta'}\right]' - \frac{r\psi'^2}{\kappa}\frac{\partial F}{\partial\delta} + \tfrac{1}{2}r^3\kappa R_0\beta' = 0 . \tag{11}$$

For a flux-conserving tokamak, the q profile is specified and ψ' is determined from

$$\psi' = \frac{r\kappa Q}{q} . \tag{12}$$

For the geometry given by Eq. (3), $Q = 1 + \bar{\kappa}/2$. Eliminating Γ' between Eqs. (8) and (10), and substituting for ψ' from (12), the system of equations (8)–(11) reduces to a set of three coupled nonlinear ordinary differential equations for σ, κ, and δ. After some lengthy but straightforward algebra, these equations can be written in the form

$$\begin{aligned} a_{11}r\sigma'' + a_{12}r^2\kappa'' + a_{13}r^2\delta'' + b_1 &= 0 , \\ a_{21}r\sigma'' + a_{22}r^2\kappa'' + a_{23}r^2\delta'' + b_2 &= 0 , \\ a_{31}r\sigma'' + a_{32}r^2\kappa'' + a_{33}r^2\delta'' + b_3 &= 0 , \end{aligned} \tag{13}$$

where $a_{11}, a_{12}, \ldots, b_3$ (given in the Appendix) are functions of r, $\beta(r)$, $q(r)$, σ', κ, $\bar{\kappa}$, δ, $r\delta'$, and averaged integrals over θ. The input β and q profiles are conveniently chosen to be of the form

$$\beta(r) = \beta_0(1 - r^2/a^2)^{\nu_1} , \tag{14}$$

$$q(r) = q_0 + (q_a - q_0)(r^2/a^2)^{\nu_2} , \tag{15}$$

where the subscripts 0 and a refer to values at the magnetic axis and plasma boundary, respectively. The boundary conditions for (13) are

$$\begin{aligned} &\sigma' = \kappa' = \delta = 0 \quad \text{at } r = 0 , \\ &\sigma = 0 , \quad \kappa = \kappa_a , \quad \delta = \delta_a \quad \text{at } r = a , \end{aligned} \tag{16}$$

where κ_a and δ_a are the elongation and triangularity of the plasma boundary. Of the total nine input parameters

(β_0, ν_1, q_0, q_a, ν_2, κ_a, δ_a, a, and R_0) not all are independent. In our formulation r is normalized by a (so that $0 \le r \le 1$), and a and R_0 occur only in combination with β_0 in the form β_0/ϵ. By using the latter as a free parameter (instead of β_0) we do not need to specify a and R_0. Equations (13) are solved numerically by employing a shooting method. A typical high-β equilibrium for a JET-type plasma boundary is shown in Fig. 1 for $\beta_0/\epsilon=0.2$, $\nu_1=1.5$, $q_0=1$, $q_a=3$, $\nu_2=2$, $\kappa_a=1.6$, and $\delta_a=0.17$.

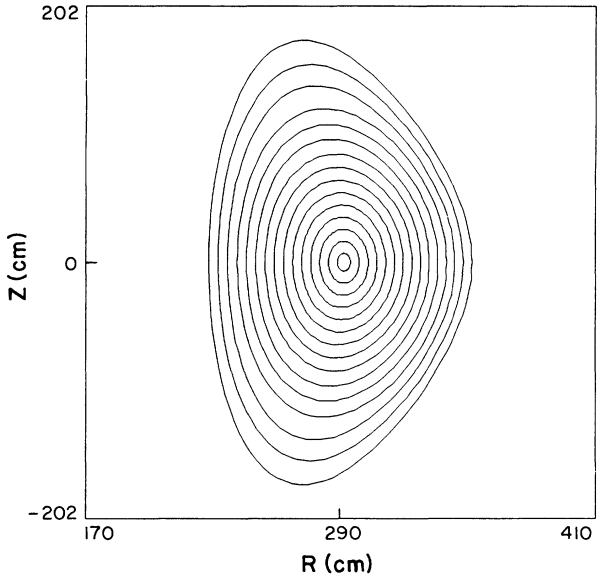

FIG. 1. Typical equilibrium flux surfaces for JET-type plasma boundary with $\beta_0/\epsilon=0.2$, $\nu_1=1.5$, $q_0=1$, $q_a=3$, $\nu_2=2$, $\kappa_a=1.6$, and $\delta_a=0.17$.

III. BALLOONING-MODE STABILITY

The linear stability of high-n ideal ballooning modes is determined by the solution of a one-dimensional eigenvalue equation derived by Connor, Hastie, and Taylor [18]:

$$\frac{d}{d\theta}\left[f\frac{d\Upsilon}{d\theta}\right]+g\Upsilon=0 , \tag{17}$$

with boundary conditions

$$\Upsilon\to 0 \quad \text{as } \theta\to\pm\infty , \tag{18}$$

where Υ is the ballooning-mode wave function and is related to the plasma displacement in the perpendicular direction, and θ is the stretched ballooning coordinate. Functions f and g are related to the equilibrium, and for our case with the geometry of the flux surfaces given by Eq. (3), they are

$$f=\frac{X}{b}(1+\Lambda^2) , \tag{19}$$

$$g=\frac{\alpha X^2}{\kappa\sqrt{b}}(R\kappa_t\Lambda-R\kappa_n)+\frac{\Omega^2X^3}{b}(1+\Lambda^2) , \tag{20}$$

$$\Lambda=\frac{b}{\kappa X^2}\left[sM+N+\frac{v}{b}X\right], \quad \Omega^2=\frac{q^2R_0^2\mu_0\rho\omega^2}{Q^2B_0^2} , \tag{21}$$

$$R\kappa_t=\frac{\sin\theta}{\sqrt{b}}, \quad R\kappa_n=-\frac{\sqrt{b}}{\kappa X}\left[\sigma'+\cos\theta-\frac{v}{b}\sin\theta\right] , \tag{22}$$

$$s=r\frac{(q/Q)'}{(q/Q)} , \tag{23}$$

$$\alpha=-\frac{q^2R_0\beta'}{Q^2} , \tag{24}$$

$$v=(\sigma'+\cos\theta)\sin\theta-\kappa^2(\cos\theta-2\delta\cos2\theta) \times[(1+\bar\kappa)\sin\theta-(\delta+\delta\bar\kappa+r\delta')\sin2\theta] , \tag{25}$$

$$M=\theta+\sigma'\sin\theta+\bar\kappa(2\theta-\sin2\theta)/4 -\delta(3\sin\theta+\sin3\theta)/3-\delta\sigma'\sin2\theta -(\delta+\delta\bar\kappa+r\delta')(3\sin\theta-\sin3\theta)/6-(\theta\to\theta_0) , \tag{26}$$

$$N=r\sigma''\sin\theta+[r^2\kappa''/\kappa+\bar\kappa(1-\bar\kappa)](2\theta-\sin2\theta)/4 -r\delta'(3\sin\theta+\sin3\theta)/3-(\delta r\sigma''+r\delta'\sigma')\sin2\theta -[\delta r^2\kappa''/\kappa+r^2\delta''+\bar\kappa(\delta-\delta\bar\kappa+r\delta')+2r\delta'] \times(3\sin\theta-\sin3\theta)/6-(\theta\to\theta_0) . \tag{27}$$

In the above, ω is the mode frequency, ρ is the mass density, s is the magnetic shear, and α is related to the pressure gradient. We define β_c, the critical parameter for the onset of ballooning instability in the first stability region, as

$$\beta_c(\%)=\langle\beta_t\rangle/\epsilon , \tag{28}$$

where

$$\langle\beta_t\rangle=\frac{\int_0^1 r\kappa(2+\bar\kappa)\beta(r)dr}{\int_0^1 r\kappa(2+\bar\kappa)dr}$$

is the volume averaged toroidal beta.

Equation (17) involves parameters α, s, σ', $r\sigma''$, κ, $\bar\kappa$, $r^2\kappa''$, δ, $r\delta'$, and $r^2\delta''$. However, using the equilibrium equations (13), $r\sigma''$, $r^2\kappa''$, and $r^2\delta''$ can be expressed in terms of the other parameters. Therefore, local stability is determined by the parameters α, s, σ', κ, $\bar\kappa$, δ, and $r\delta'$. We carry out a detailed parametric study of the effect of these quantities on the first and second stability boundaries in the s-α plane. For the numerical solution of Eq. (17) we again employ a shooting method. Our results on the local and global stabilities of ballooning modes are discussed in Sec. IV. Following Sykes, Turner, and Patel [11] and Troyon *et al.* [1], we also use the cylindrical safety factor $q_c=2AB/(R_0I_p)$ (where A is the plasma cross section area, B the toroidal magnetic field, and I_p the plasma current) instead of q_a to express our results in order to make the comparison easier with their work. It should be noted that in our analysis we use rigid pressure profiles to determine the maximum value of β_c for the ballooning stability. The assumption of rigid pressure profiles is a simplification based on earlier observations [16,17] that the error made in the β limit as compared to that obtained using an optimized profile is not very significant. However, use of a rigid profile does make our β-limit value a conservative one.

IV. RESULTS AND DISCUSSION

A. Local stability analysis

For the local stability analysis, marginal stability boundaries are obtained on a given flux surface, and their variation with the equilibrium parameters σ', κ, $\bar{\kappa}$, δ, and $r\delta'$ are studied. Figure 2 shows a representative s-α diagram where, keeping all other parameters fixed ($\sigma'=\bar{\kappa}=-0.4$, $\kappa=1$, $r\delta'=0$), δ is varied in the range (-0.2 to 0.2). In this particular case, it is seen that positive triangularity has a stabilizing effect, while negative triangularity has a destabilizing effect on the first stability boundary. Typically our results from local stability analysis indicate that for input parameters belonging to a realistic equilibrium the effect of triangularity of the flux surface is usually stabilizing only for low magnetic shear cases (e.g., for a typical JET plasma equilibrium, δ stabilizes the first boundary when $s \leq 1.2$).

The effect of triangularity (for both positive and negative values of δ) on the first stability boundary is found to be generally destabilizing when σ' and κ' are negative (a small stabilizing effect is observed for only the $\kappa=1$ and $\delta>0$ case). However, when $\sigma'<0$ and $\kappa'>0$ the effect of $\delta>0$ is found to be stabilizing for $\kappa>1$ cases. $\delta'>0$ usually enhances this stabilizing effect. The occurrence of these combinations ($\sigma'<0,\kappa'<0$) and ($\sigma'<0,\kappa'>0$) on the equilibrium surfaces, are found to depend on the values of the boundary elongation, namely $\kappa_a<1.3$ and $\kappa_a>1.5$ respectively. As we will see later, the global stability results (Fig. 4) are consistent with these results.

B. Global stability analysis

On the basis of the local stability analysis discussed above, it is possible to obtain a global marginal stability boundary and to compute β_c defined in Eq. (28) as a function of κ_a, δ_a, and q_c. Briefly, the procedure is as follows. Following the solution of Eq. (13) to obtain profiles of equilibrium parameters, Eq. (17) is solved for ω^2, and stability is tested on a number of flux surfaces (usually 20 surfaces equally spaced in the minor radius direction). If all surfaces are found to be stable, then β_0/ϵ is raised (otherwise it is lowered) and the stability tests are repeated until at least one flux surface becomes ballooning unstable. The last value of β_0/ϵ (determined with a maximum error of 1%) for which all surfaces are stable corresponds to the global marginal stability boundary. The critical β_c is then calculated using Eq. (28). This yields one point on the global stability diagram. Following such a procedure, we have examined the global stability boundary as a function of elongation, triangularity, and q_c. In Fig. 3 we plot β_c versus q_c for various values of κ_a and δ_a using the scaling law Eq. (29) (numerically calculated values of β_c are shown by different symbols). The curves in the solid lines correspond to $\kappa_a=1$ and $\delta_a=0,0.15$ and clearly show the destabilizing effect of triangularity for all values of q_c. The plots in dash-dots and dots correspond to $\kappa_a=1.6$ and 2, respectively, and exhibit a stabilizing effect from triangularity. This figure also shows that β_c depends weakly on the plasma shape for larger q_c. For $\kappa_a \leq 1.6$ and $\delta_a=0$, β_c depends rather weakly on q_c, but this dependence notably increases for the $\kappa_a=2$ and $\delta_a=0.2$ cases. In Fig. 4 we have consolidated a large number of our results to schematically show that the effect of δ_a on the stability depends not only on κ_a but also on q_c (e.g., for $\kappa_a=1.5$, the effect is destabilizing for $q_c=2.3$ but stabilizing otherwise). For $\kappa_a \geq 1.6$, triangularity always increases β_c irrespective of the q_c

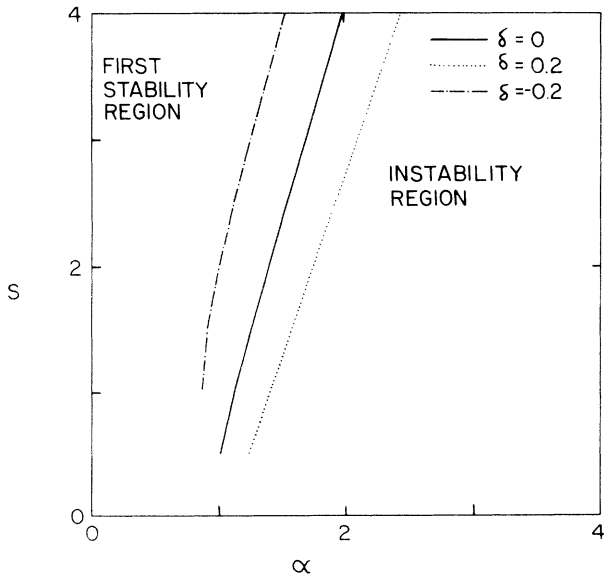

FIG. 2. Representative s-α diagram for local ballooning stability showing the stabilizing effect of the positive triangularity on the first (marginal) stability boundary ($\sigma'=\bar{\kappa}=-0.4$, $\kappa=1$, $r\delta'=0$, and $\delta=0,\pm0.2$).

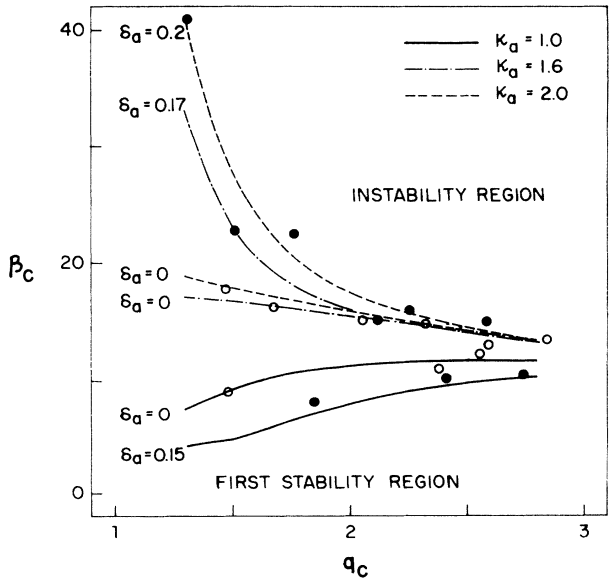

FIG. 3. Global stability diagrams for the high-β tokamak showing the marginal stability boundaries in the β_c-q_c plane as κ_a and δ_a change for $q_0=1$, $\nu_1=1.5$, and $\nu_2=2$ (solid lines: $\kappa_a=1$, $\delta_a=0,0.15$; dash-dotted lines: $\kappa_a=1.6$, $\delta_a=0,0.17$; dotted lines: $\kappa_a=2$, $\delta_a=0,0.2$).

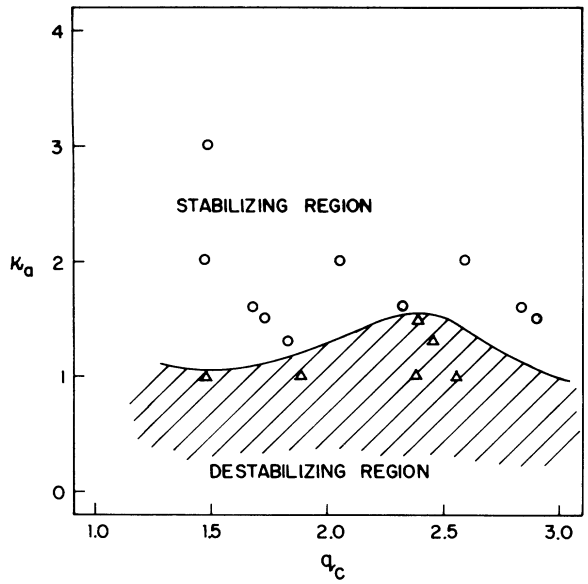

FIG. 4. A schematic diagram showing the effect of plasma boundary triangularity δ_a on the stability of high-n ideal ballooning modes in the κ_a-q_c plane.

value. In Fig. 5 we show that for $\delta_a=0$ the boundary elongation always increases the stabilization for all q_c values. The same effect is also observed by Mauel [17] for $\delta(r)=0$. Note that there is a turnover at $\kappa_a \approx 1.25$, indicating a change in the dependence of β_c on q_c.

Based on our numerical results we have also obtained a generalized scaling law for the high-n ideal ballooning β limit in terms of parameters κ_a, δ_a, and q_c. It is given by

$$\beta_c = 88\kappa_a^{-0.6} q_c^{-0.81}[1-0.974\kappa_a^{-0.6} q_c^{-0.33}] + 973\kappa_a^{-0.4} q_c^{-4.66}\delta_a[1-2.158\kappa_a^{-1.3} q_c^{-0.9}\delta_a^{0.5}] \quad (29)$$

and is valid over the following range of parameters: $1 \le \kappa_a \le 2$, $0 \le \delta_a \le 0.2$, and $1.3 < q_c < 2.8$. The scaling law (29) effectively captures all the qualitative dependences of β_c discussed above and shown in Figs. 3–5. It should be noted that in the limits of small κ_a, small q_c ($\kappa_a=1$, $q_c=2$) and large κ_a, large q_c ($\kappa_a=2$, $q_c=4$), the scaling law also reproduces the qualitative features of the scaling law of Sykes, Turner, and Patel [11]. As extensively discussed in [19], one of the inherent difficulties of deriving scaling laws from statistical regression analysis is that they are nonunique (i.e. for the same value of minimum χ^2 there can be a number of scaling laws with different exponents). Keeping that in mind, we have chosen the scaling law that best captures the various qualitative features of our analysis, as well as has the least χ^2 error. In deriving Eq. (29), the q value at the magnetic axis (q_0) and the profile shape parameters in the β and q profiles kept fixed ($q_0=1$, $\nu_1=1.5$, $\nu_2=2$). We have used a mixed method for determining the unknowns in the scaling law in order to minimize the χ^2 error. A linear least-squares fitting method is used to determine the linear coefficients in the scaling law, while the unknown exponents are determined by using a shooting method. It should be noted that the maximum absolute error in determining β_c (the maximum value in the first stability region) numerically is 0.4 and the average χ^2 error in fitting is 0.7. Figure 6 shows the plot of numerical values of β_c, and those predicted from the scaling law using Eq. (29). The agreement is seen to be quite good. A numerical study of the dependence of q_c on q_a, κ_a, and δ_a shows that q_c varies approximately linearly with q_a in general for all plasma shapes, and the slope of the straight line depends weakly on the plasma shape.

We have also studied the effect on β_c due to variations in the shape of β and q profiles given by Eqs. (14) and (15) by changing the exponents ν_1 and ν_2 for a JET-type plas-

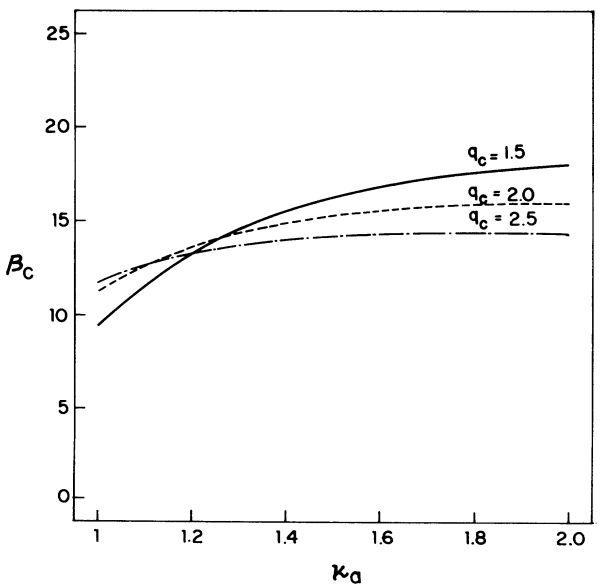

FIG. 5. Plot showing the dependence of β_c on the elongation κ_a and q_c when $\delta_a=0$.

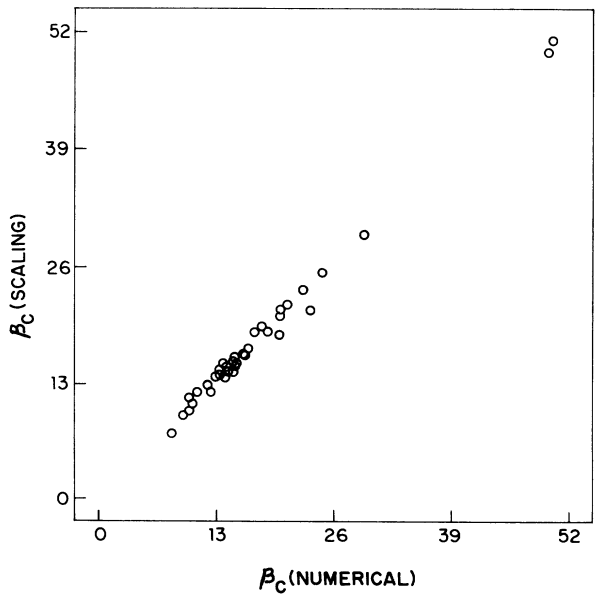

FIG. 6. Numerical β_c vs. β_c as calculated from the derived scaling law.

TABLE I. Influence of ν_1 and ν_2 on the ballooning beta limit β_c (in %).

ν_1	$\nu_2=1$	$=2$	$=3$
0.5	40	41	60
1.5	19	24	28
3.0	11	17	24

ma boundary. The dependence of β_c on the parameters ν_1 and ν_2 for $q_a=2$, $\kappa_a=1.6$, and $\delta_a=0.17$ is shown in Table I. β_c decreases with ν_1 and increases with ν_2. It takes a maximum value ($\beta_c=60\%$) for $\nu_1=0.5$ and $\nu_2=3$. This indicates that a broad β profile and a q profile with low central shear and high edge shear appear favorable for achieving a high-β_c value.

To summarize, we find that the effect of κ_a is always stabilizing, while the effect of δ_a on β_c depends on κ_a and q_c. For $\kappa_a>1.6$, the effect of δ_a is stabilizing for all q_c values (in the range 1.2–3). These results are consistent with earlier findings in [8–10]. The improvement in stability is significantly large for high elongation and small q_c. For a circular boundary ($\kappa_a=1$) the effect of δ_a is always destabilizing. A study of the dependence of β_c on β and q profile shapes indicates that broad β profiles and q profiles with sharper gradients in the edge region are favorable. Our results are expressed in a scaling law which reveals the detailed dependence on elongation, triangularity, and cylindrical safety factor for a wide range of parameters.

APPENDIX

The coefficients $a_{11}, a_{12}, \ldots, b_3$ in Eq. (13) are given by

$$a_{11}=g_{21},\quad a_{12}=g_{22}+f_1h_5,\quad a_{13}=g_{23},$$
$$a_{21}=g_{31}+f_3g_{11},\quad a_{22}=g_{32}+f_3g_{12}+f_4h_5,$$
$$a_{23}=g_{33}+f_3g_{13},\quad a_{31}=g_{41},\quad a_{32}=g_{42}+f_6h_5,$$
$$a_{33}=g_{43},\quad b_1=h_2+f_1h_6+f_2,$$
$$b_2=h_3+f_3h_1+f_4h_6+f_5,\quad b_3=h_4+f_6h_6+f_7,$$

where

$$f_1=\frac{2}{Q}\frac{\partial F}{\partial\sigma'},\quad f_2=(3+\bar\kappa-2rq'/q)\frac{\partial F}{\partial\sigma'}-\frac{q^2R_0\beta'}{Q^2},$$

$$f_3=\frac{2}{\kappa(2+\bar\kappa)},\quad f_4=\frac{2}{Q}\left[\frac{1}{r}\frac{\partial F}{\partial\kappa'}+\frac{F}{\kappa(2+\bar\kappa)}\right],$$

$$f_5=(4+\bar\kappa-2rq'/q)\frac{1}{r}\frac{\partial F}{\partial\kappa'}+\frac{2}{\kappa(2+\bar\kappa)}(2-rq'/q)F-\frac{\partial F}{\partial\kappa}+\frac{F}{\kappa}+\left[\frac{\sigma'-(\delta+r\delta')/2}{\kappa(2+\bar\kappa)}\right]\frac{q^2R_0\beta'}{Q^2},$$

$$f_6=\frac{2}{Q}\left[\frac{1}{r}\frac{\partial F}{\partial\delta'}\right],$$

$$f_7=(4+\bar\kappa-2rq'/q)\frac{1}{r}\frac{\partial F}{\partial\delta'}-\frac{\partial F}{\partial\delta}+\frac{1}{2}\frac{q^2R_0\beta'}{Q^2},$$

$$g_{ij}=\langle\phi_i\xi_j\rangle_\theta,$$

$$\langle\cdots\rangle_\theta=\frac{1}{2\pi}\int_0^{2\pi}(\cdots)d\theta,\quad i=1,2,3,4,\quad j=1,2,3,$$

$$\phi_1=-\frac{b}{X^2},\quad \phi_2=\frac{2b}{X^3}(\cos\theta-2\delta\cos2\theta),$$

$$\phi_3=\frac{2b}{X^3}(\sin\theta-\delta\sin2\theta)(\sin\theta/\kappa),$$

$$\phi_4=-\frac{2b}{X^3}\sin\theta\sin2\theta,$$

$$\xi_1=\cos\theta-2\delta\cos2\theta,\quad \xi_2=(\sin\theta-\delta\sin2\theta)\sin\theta/\kappa,$$

$$\xi_3=-\sin\theta\sin2\theta,$$

$$\xi_4=\bar\kappa(1-\bar\kappa)\sin^2\theta-2r\delta'(\cos\theta+\sigma'\cos2\theta)-\bar\kappa(\delta+r\delta'-\delta\bar\kappa)\sin\theta\sin2\theta,$$

$$h_1=\langle-b\xi_4/X^2+rb'/X\rangle_\theta,$$

$$h_2=\left\langle\left[\frac{2b}{X^3}\xi_4-\frac{rb'}{X^2}\right](\cos\theta-2\delta\cos2\theta)+\frac{2br\delta'}{X^2}\cos2\theta\right\rangle_\theta,$$

$$h_3=\left\langle\left[\frac{2b}{X^3}\xi_4-\frac{rb'}{X^2}\right](\sin\theta-\delta\sin2\theta)(\sin\theta/\kappa)+\frac{b}{X^2}\frac{[\bar\kappa\sin\theta+(r\delta'-\delta\bar\kappa)\sin2\theta]\sin\theta}{\kappa}\right\rangle_\theta,$$

$$h_4=\left\langle-\frac{2b}{X^3}\xi_4\sin\theta\sin2\theta+\frac{rb'}{X^2}\sin\theta\sin2\theta\right\rangle_\theta,$$

$$h_5=\frac{1}{2\kappa},\quad h_6=\tfrac{1}{2}\bar\kappa(1-\bar\kappa),$$

$$rb'=2\kappa^2(\cos\theta-2\delta\cos2\theta)\{\bar\kappa(\cos\theta-2\delta\cos2\theta)-2r\delta'\cos2\theta\},$$

$$\frac{\partial F}{\partial\sigma'}=-\left\langle\frac{b}{X^2}(\cos\theta-2\delta\cos2\theta)\right\rangle_\theta,$$

$$\frac{\partial F}{\partial\kappa}=\left\langle\frac{2\kappa}{X}(\cos\theta-2\delta\cos2\theta)^2+\frac{b}{X^2}\frac{\bar\kappa\sin\theta}{\kappa}(\sin\theta-\delta\sin2\theta)\right\rangle_\theta,$$

$$\frac{1}{r}\frac{\partial F}{\partial\kappa'}=-\left\langle\frac{b}{X^2}(\sin\theta-\delta\sin2\theta)(\sin\theta/\kappa)\right\rangle_\theta,$$

$$\frac{\partial F}{\partial\delta}=\left\langle-4\kappa^2\cos2\theta(\cos\theta-2\delta\cos2\theta)/X+(b/X^2)\{2\cos2\theta(\sigma'+\cos\theta)+(1+\bar\kappa)\sin\theta\sin2\theta\}\right\rangle_\theta,$$

$$\frac{1}{r}\frac{\partial F}{\partial\delta'}=\left\langle\frac{b}{X^2}\sin\theta\sin2\theta\right\rangle_\theta.$$

(F, b, X, Q are given in Sec. II.)

[1] F. Troyon, R. Gruber, H. Saurenmann, S. Semenzato, and S. Succi, Plasma Phys. Contr. Fusion **26**, 209 (1984).
[2] J. P. Freidberg, *Ideal Magnetohydrodynamics* (Plenum, New York, 1987).
[3] B. Coppi, A. Ferreira, J. W. K. Mark, and J. J. Ramos, Nucl. Fusion **19**, 715 (1979).
[4] J. R. Ferron *et al.*, in *Controlled Fusion and Plasma Heating, Proceedings of the 17th European Conference Geneva, 1990,* edited by G. Briffod, Adri Nijsen-Vis, and F. C. Schüller (European Physical Society, Petit-Lancy, Switzerland, 1990), Part I, p. 371.
[5] P. Smeulders *et al.*, in Ref. [4], p. 323
[6] O. J. Kwon and T. C. Hender, Plasma Phys. Contr. Fusion **34**, 273 (1992).
[7] E. A. Lazarus *et al.*, Phys. Fluids B **3**, 2220 (1991).
[8] G. Eriksson, A. Bondeson, D. J. Ward, F. Hofmann, and L. Villard, in *Proceedings of the International Conference on Plasma Physics, Innsbruck, 1992,* edited by W. Freysinger, K. Lackner, R. Schrittwieser, and W. Lindinger (European Physical Society, Petit-Lancy, Switzerland, 1992), Vol. 16C, Part I, p. 343.
[9] G. Schultz, A. Bondeson, F. Troyon, and A. Roy, in *Plasma Physics and Controlled Nuclear Fusion Research, Proceedings of the 13th International Conference, Washington, 1990* (IAEA, Vienna, 1991), Vol. 2, p. 101.
[10] M. W. Phillips, A. M. M. Todd, M. H. Hughes, J. Manickam, J. L. Johnson, and R. R. Parker, Nucl. Fusion **28**, 1499 (1988).
[11] A. Sykes, M. F. Turner, and S. Patel, in *Controlled Fusion and Plasma Physics, Proceedings of the 11th European Conference, Aachen, 1983* (European Physical Society, Petit-Lancy, Switzerland, 1983), Vol. 7D, Part II, p. 363.
[12] T. Tuda *et al.*, in *Plasma Physics and Controlled Nuclear Fusion Research, Proceedings of the 10th International Conference, London, 1984* (IAEA, Vienna, 1985), Vol. 2, p. 173.
[13] L. C. Bernard, F. J. Helton, R. W. Moore, and T. N. Todd, Nucl. Fusion **23**, 1475 (1983).
[14] A. K. Agarwal *et al.*, in Ref. [9], Vol. 2, p. 247.
[15] A. K. Agarwal, S. N. Bhattacharyya, and A. Sen, Plasma Phys. Contr. Fusion **34**, 1211 (1992).
[16] W. H. Choe and J. P. Freidberg, Phys. Fluids **29**, 1766 (1986).
[17] M. E. Mauel, Phys. Fluids **30**, 3843 (1987).
[18] J. W. Connor, R. J. Hastie, and J. B. Taylor, Phys. Rev. Lett. **40**, 396 (1978).
[19] P. N. Yushmanov, T. Takizuka, K. S. Riedel, O. J. W. F. Kardaun, J. G. Cordey, S. M. Kaye, and D. E. Post, Nucl. Fusion **30**, 1999 (1990).